

## Optical modulational instability in a nonlocal medium

Marco Peccianti, Claudio Conti, and Gaetano Assanto

*NOOEL–Nonlinear Optics and Optoelectronics Laboratory, National Institute for the Physics of Matter, INFN–Roma Tre,  
Via della Vasca Navale 84, 00146 Rome, Italy\**

(Received 21 February 2003; published 12 August 2003)

We report the first observation of modulational instability in nematic liquid crystals encompassing a nonlocal behavior. The experimental results are quantitatively compared with the theory revealing the fundamental features associated to a nonlocal nonlinearity.

DOI: 10.1103/PhysRevE.68.025602

PACS number(s): 42.65.Tg, 42.65.Jx, 42.70.Df

Plane-wave Fourier components of an arbitrary excitation travel independently in a linear homogeneous medium. When a nonlinear response has to be accounted for, coupling and, therefore, energy redistribution between such Fourier components takes place and is often referred to as modulational instability (MI). The nonlinearly induced coupling is not spectrally flat but, depending on the specific process and configuration, yields maximum gain at and around a spatial frequency, i.e., a specific periodic modulation tends to prevail on the others upon propagation. While the periodic perturbation is usually extracted from noise, its amplification is carried out at the expense of a pump wave and can trigger some other nonlinear effects, among them is the formation of several spatial solitons out of a broad-beam excitation. As the triggering mechanism of complex nonlinear behaviors, MI has steered renewed interest in several areas of nonlinear sciences, including solitons in discrete and dissipative media [1], matter waves in Bose-Einstein condensates (BEC) [2], and optical patterns in resonators [3]. While MI provides an elegant approach to the generation of pulse trains in optical fibers [4], and plays a key role in hydrodynamics and plasma physics [5–7], in the optical spatial domain it was originally explored with reference to Kerr media [8], and has been recently investigated in diverse materials [9–16].

Following the original contribution by Litvak in plasmas [17] and the attention devoted to nonlocality [18] in photorefractive [19–21], thermo-optic [22], liquid crystalline [23,24] media and in BEC [25,26], optical MI in nonlocal nonlinear systems (NL-MI) has recently been the subject of theoretical investigations [27,28]. However, thus far no experimental (quantitative) evidence of NL-MI has been reported in literature.

The simplest form of optical MI takes place via a local, self-focusing, Kerr nonlinearity, i.e., where the optical intensity punctually (in time or in space) modifies the refractive index distribution and, consequently, the wave propagation. In the spatial case, e.g., for spatially modulated continuous-wave beams, a local perturbation in refractive index can undergo amplification at the expense of a pump beam, rendering plane waves unstable to long-wavelength sideband modulations. If sufficient energy is available in the pump, there is no limitation to the spatial frequency that can be amplified. Conversely, if the medium is nonlocal, the optical

intensity at a given location modifies the refractive distribution in a finite-size region. For this reason NL-MI strongly differs from the local case, the most remarkable effect being the spatial filtering of the amplified harmonics and, hence, the flattening and narrowing of the MI gain profile. In a nonlocal material, in fact, the frequency-domain coupling due to the nonlinear response is accompanied by the physical-domain coupling due to the nonlocality, thereby limiting the energy transfer from the pump to higher harmonics and resulting in an overall reduction of NL-MI effects compared to Kerr MI.

In this paper, for the first time to the best of our knowledge, we report experimental evidence and quantitative measurements of MI in a regime markedly defined by nonlocality. The experiments were carried out in a nematic liquid crystal (LC) cell, with the setup and the geometry sketched in Fig. 1. A linearly polarized laser beam was injected into a planar-interface glass cell containing an undoped nematic LC. The LC was properly anchored and voltage biased to guarantee a preset orientation of its molecular director, while the beam evolution could be monitored with an optical microscope and a camera imaging the out-of-plane scattered light. An input glass interface, parallel to  $X$ , prevented the occurrence of undesired depolarization effects. The aligned liquid crystal, anchored at the boundaries, behaves as a positive uniaxial with  $n_{\parallel} = n_z$  and  $n_{\perp} = n_x$ . In the presence of an external quasistatic (electric or magnetic) field or specific anchorage at the interfaces, the refractive index  $n(\theta)$  in the

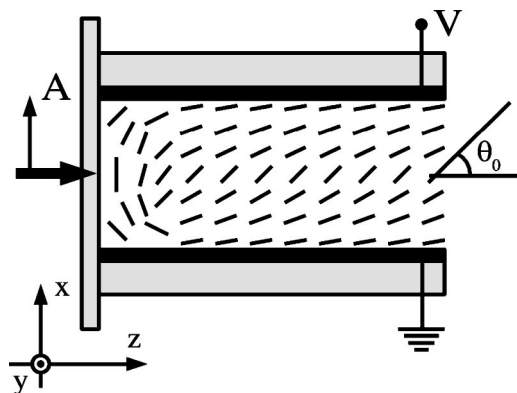


FIG. 1. Experimental setup: a planar glass cell containing an undoped nematic LC with a preset orientation of its molecular director. A camera retrieves the scattered light from the top of the cell.

\*URL: [http://optow.ele.uniroma3.it/opto\\_2002.shtml](http://optow.ele.uniroma3.it/opto_2002.shtml)

( $X, Z$ ) principal plane can exhibit a distribution  $\hat{\theta}(X)$ , with  $n_{\perp} < n[\hat{\theta}(X)] < n_{\parallel}$  [29,30]. Given an optical beam excitation of envelope  $A$ , linearly-polarized along  $X$  and propagating along  $Z$ , being  $\theta(X, Y, Z) = \hat{\theta}(X) + [\hat{\theta}(X)/\theta_0]\Psi(X, Y, Z)$  the angular distribution of the director, and  $\theta_0$  is the displacement in the middle of the cell (i.e., near the beam axis), if the beam transverse size is well below the cell thickness  $L$  and vectorial effects can be neglected, at the first order in  $|A|^2$  and  $\Psi$  the relevant equations can be cast as [31]

$$2ik_0 n \partial_z A + \nabla_{\perp}^2 A + k_0^2 n_a^2 \sin(2\theta_0) \Psi A = 0,$$

$$K \nabla^2 \Psi - \Delta \epsilon_{RF} E^2 \frac{\sin(2\theta_0)}{2\theta_0} (1 - \gamma_0) \Psi + \frac{\epsilon_0 n_a^2}{4} \sin(2\theta_0) |A|^2 = 0, \quad (1)$$

where  $k_0$  is the vacuum wave number,  $n_a^2 = n_{\parallel}^2 - n_{\perp}^2$  the optical anisotropy,  $k^2 = k_0^2 [n_{\perp}^2 + n_a^2 \sin^2(\theta_0)]$ .

In Eq. (1)  $\gamma_0 = 2\theta_0 \cos(2\theta_0)/\sin(2\theta_0)$  quantifies the deviation from the condition of maximum nonlinear response at  $\theta_0 = \pi/4$  (e.g.,  $\gamma_0 = 0$  when  $\theta_0 = \pi/4$ ). In the experiments, the latter can be controlled by varying the applied voltage across  $L$ .

It is instructive to write Eq. (1) in a dimensionless form by setting  $A = (A_c/\alpha) a(R/R_c, Z/\alpha Z_c) \exp(iZ/\alpha Z_c)$ ,  $\Psi = (\Psi_c/\alpha) \psi(R/R_c, Z/\alpha Z_c)$  with  $A_c^2 = \Delta \epsilon_{RF}^2 E^4 / 2\theta_0^2 \epsilon_0 k_0^2 n_a^4 K$ ,  $R_c^2 = 2\theta_0 K / \sin(2\theta_0) \Delta \epsilon_{RF} E^2$ ,  $\Psi_c = \Delta \epsilon_{RF} E^2 / 2\theta_0 k_0^2 n_a^2 K$ , and  $Z_c = 2kR_c^2$ ,  $\epsilon = \sin(2\theta_0) \Delta \epsilon E^2 / 2\theta_0 k_0^2 n^2 K$ .

We then obtain

$$i \frac{\partial a}{\partial z} + \nabla_{\perp}^2 a - a + a \psi = 0, \quad (2)$$

$$\frac{\epsilon}{\alpha} \frac{\partial^2 \psi}{\partial z^2} + \nabla_{\perp}^2 \psi - \alpha(1 - \gamma_0) \psi + \frac{1}{2} |a|^2 = 0,$$

with  $\alpha$  real positive parameter, the role of which is addressed below.

We have recently shown that Eqs. (2), in a wide range of experimental conditions (when  $\epsilon \cong 0$ ), support stable self-trapped beams characteristic of ‘‘highly nonlocal media.’’ [18,31] Here we discuss NL-MI, both theoretically and experimentally, in the one-dimensional case (i.e., for  $\partial_x = 0$ ) employing a configuration with an elongated (along  $y$ ) Gaussian beam input. Taking  $\epsilon = 0$  and  $\partial_x = 0$ , Eq. (2) reduce to:

$$i \partial_z a + \partial_{yy} a - a + a \psi = 0, \quad (3)$$

$$\partial_{yy} \psi - \alpha(1 - \gamma_0) \psi + \frac{1}{2} |a|^2 = 0.$$

In this context,  $\alpha > 0$  identifies the plane-wave solution (sometime referred to as the ‘‘nonlinear eigenmode’’ [15]), which is unstable with respect to sideband modulations:  $\psi = 1$ ,  $a = \sqrt{2\alpha(1 - \gamma_0)}$  (hereafter  $\gamma_0 < 1$ ).

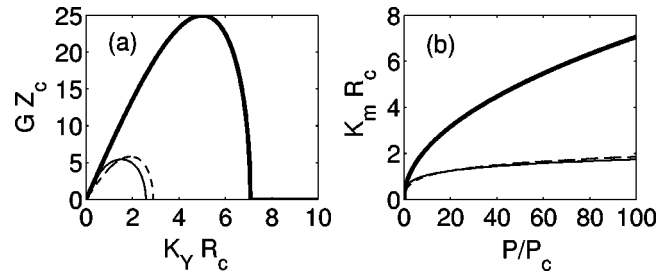


FIG. 2. (a) MI gain for a local Kerr (thick solid) and a nonlocal LC medium with  $\theta_0 = \pi/4$  (thin solid) and  $\theta_0 = \pi/3$  (dashed). (b) Maximally amplified spatial harmonic for a local Kerr (thick solid) and nonlocal LC's with  $\theta_0 = \pi/4$  (thin solid) and  $\theta_0 = \pi/3$  (dashed).

The pertinent NL-MI belongs to the family of the ‘‘exponential response functions,’’ originally studied by Litvak [17] and investigated in detail in Refs. [27,28]. A spatial harmonic perturbation with transverse wave vector  $k_y$  grows exponentially along propagation, the related gain is given by  $\exp(gz)$ , with

$$g(k_y) = |k_y| \sqrt{\frac{2\alpha(1 - \gamma_0)}{\alpha(1 - \gamma_0) + k_y^2} - k_y^2}. \quad (4)$$

The corresponding Kerr-like expression is readily obtained in the limit  $\alpha \rightarrow \infty$ :  $g_K(k_y) = |k_y| \sqrt{2 - k_y^2}$ . In fact,  $\alpha$  quantifies the *degree of nonlocality* and directly measures the beam fluence. After simple inspection, Eq. (4) immediately reveals that, in the nonlocal case, the high frequency gain is limited by the filtering due to spatial-domain coupling.

Using real-world (MKS) units, the NL-MI amplification is given by  $\exp[G(K_Y)Z]$ , with  $K_Y$  the harmonic wave number in  $m^{-1}$  and

$$G(K_Y) = \frac{|K_Y| R_c}{Z_c} \sqrt{\frac{P}{P_r} \frac{1}{1 - \gamma_0 + (K_Y R_c)^2} - (K_Y R_c)^2}. \quad (5)$$

Note that in Eq. (5)  $R_c$  and  $Z_c$  are reference lengths that only depend on material parameters and  $\theta_0$ , while  $P_r$  is a reference power. Since the power actually injected into the LC is undetermined *a priori* because of the complicated coupling at the input interface of the cell,  $P_r$  can be used as a fitting parameter.

For the sake of comparison, in the equivalent local medium the corresponding gain profile is

$$G_K(K_Y) = \frac{|K_Y| R_c}{Z_c} \sqrt{\frac{P}{P_r} - (K_Y R_c)^2}. \quad (6)$$

Note that, in deriving expressions (5) and (6), we made the standard hypothesis (as in the experiments) that a plane wave is well approximated by a wide elliptical Gaussian beam of power  $P$ .

In Fig. 2 we show the MI gain versus wave number and the position of the most amplified spatial harmonic  $K_m$  versus power (corresponding to the maximum of  $G$ ), comparing

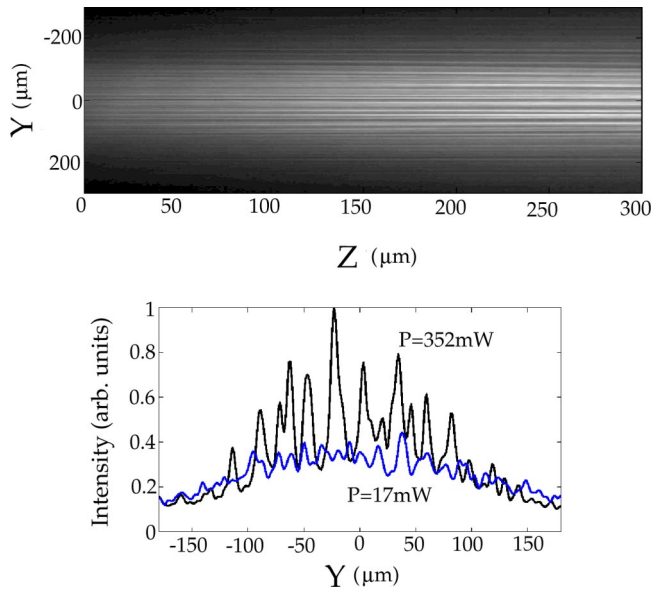


FIG. 3. (Top) Spatial intensity along  $Z$  for  $P=352$  mW. (Bottom) Intensity profiles vs  $Y$  for two different powers at  $Z \cong 300$   $\mu\text{m}$ .

Kerr and nonlocal cases. For the former MI is much more pronounced, while for the latter the maximum gain is approximately independent of power at large fluences. We stress that the NL-MI features are only marginally affected (within experimental errors) by the specific value of  $\theta_0$ . The latter can be voltage adjusted with good accuracy around  $\pi/4$ , corresponding to the most pronounced nonlinear response [30].

In the experiments, we employed a wide (along  $Y$ ) Gaussian beam incident onto the LC cell from an Argon-ion laser operating cw at  $\lambda = 514.5$  nm. The PVA-coated planar interfaces anchored the LC director with a small tilt, as to prevent the formation of reorientational domains and disclinations (see Fig. 1). The nematic LC was the commercial E7 mixture, characterized by  $K=9 \times 10^{-12}$  N,  $\Delta\epsilon_{RF}=14.5\epsilon_0$ ,  $n_{\perp}=1.5$ ,  $n_a=0.9$ , being  $\epsilon_0$  the vacuum permittivity and  $E=V/L$ , with  $V=1.62$  V the applied radio frequency voltage and  $L=75$   $\mu\text{m}$ . For such values,  $\epsilon \cong 3 \times 10^{-6}$ . The fluctuations due to spatial noise seeded the NL-MI, and the corresponding images in the  $Y$ - $Z$  plane were acquired with the digital camera and, subsequently, numerically analyzed and processed.

Figure 3 shows the experimental evidence of NL-MI: upon propagation and superimposed to the wide input beam, a periodic pattern emerges and is progressively amplified. The transverse intensity profile at  $Z=300$   $\mu\text{m}$  is reported for two different input powers: the periodic modulation is apparent and corresponds to a low-frequency MI gain as in Fig. 2. It is worth underlining that we focus on the initial stage of beam propagation, where the modulational instability can be effectively treated using a perturbative approach and, hence, according to the theory above.

In order to characterize quantitatively the NL-MI process, from the digitally acquired data of the transverse beam-intensity profile (along  $Y$ ), we calculated the square moduli

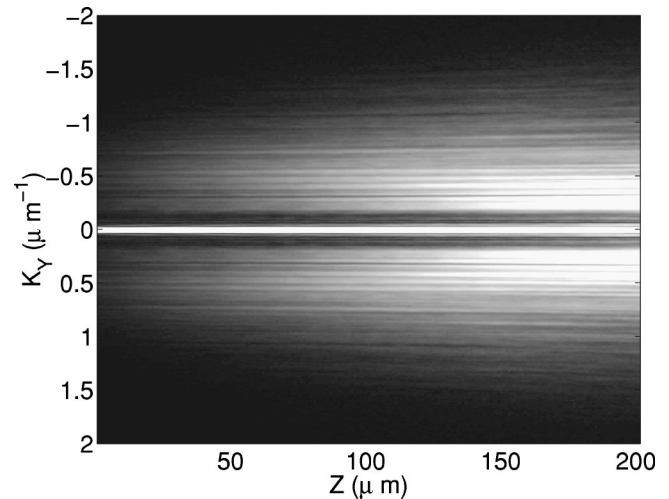


FIG. 4. Spectrum of the optical intensity vs  $Z$ , corresponding to the top panel of Fig. 3 (time-averaged FFT of camera snapshots).

of the time-averaged (in order to filter out fluctuations) fast fourier transform (FFT), as reassembled in Fig. 4. The side-band modulation growing in amplitude and visibility along the propagation coordinate  $z$  is apparent, and so is the onset of NL-MI.

For two representative powers of 18 and 185 mW, respectively, Fig. 5 shows the details of the corresponding FFT's in  $Z \cong 100$   $\mu\text{m}$ . Subtracting from each spectrum the corresponding one obtained at low excitation (i.e., in the linear regime), we eliminated the background noise in order to better emphasize shape and position of the NL-MI bandwidth. Finally, via low-pass filtering, we could determine the position of the maximally amplified harmonic, as displayed in Fig. 6 versus power. The data shown refer to two distinct values of  $Z$ , providing the same  $K_m$  (within experimental error) as predicted by the linearized MI analysis. Such processed data were compared with calculations from Eq. (5), the only fitting parameter being  $P_r$  and assuming  $\theta_0 = \pi/4$  within reasonable approximation. Minimization of the stan-

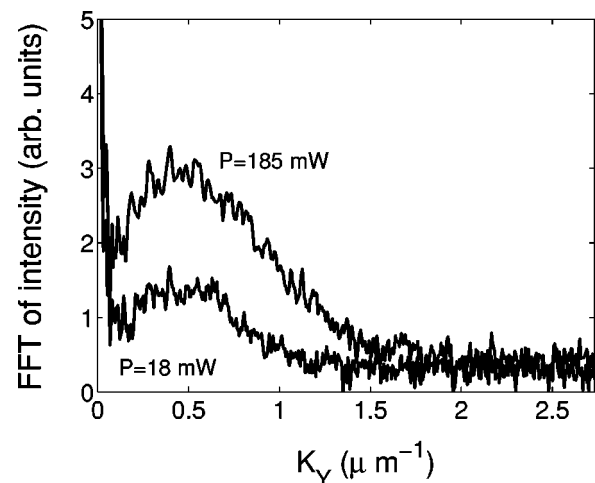


FIG. 5. FFT of intensity at  $Z \cong 100$   $\mu\text{m}$  for two different powers in the cell.

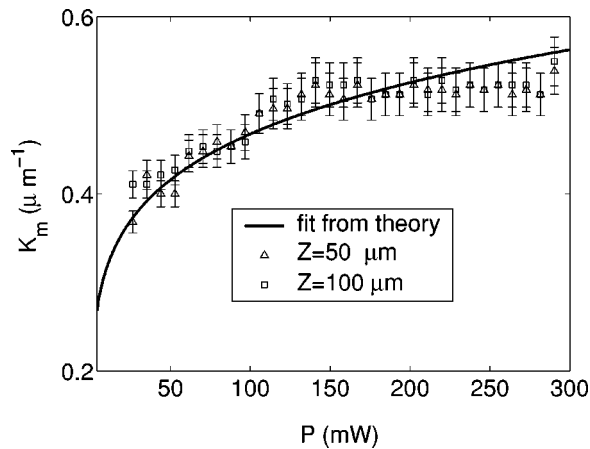


FIG. 6. Maximally amplified spatial harmonic vs power: squares, experimental data at  $Z \cong 100 \mu\text{m}$ ; triangles, experimental data at  $Z \cong 50 \mu\text{m}$ ; solid line, fit from the theory.

standard deviation between calculations and experimental data yielded  $P_r = 0.4 \mu\text{W}$ .

The mean error, defined as  $\sqrt{|1 - (\text{theoretical})/(\text{measured})|^2}$  with the average calculated over power, is 4%. As expected, at high fluences (i.e.,

at powers above 200 mW) the linear theory of MI provides less accurate estimates of  $K_m$ .

One can compare these results with the corresponding ones stemming from the Kerr expression for the gain. The latter overestimates  $K_m$  by nearly two orders of magnitude. Only in a few instances a detailed relationship between periodicity and beam fluence has been explored experimentally and compared with the theory (see, e.g., Refs. [14,15]). By using  $P_r$  in Eq. (5), the derived NL-MI gain in our sample is more than two orders of magnitude greater than the MI gain evaluated by Schiek *et al.* in the electronic parametric case [15]. This is in qualitative agreement with both the size of the reorientational nonlinearity in LC's [29,30] and the role played by the nonlocality.

In conclusion, we have characterized the phenomenon of transverse modulational instability in a highly nonlocal material, namely, a nematic liquid crystal. The quantitative comparison with theory confirms the existence of one-dimensional NL-MI and the distinctive role of nonlinear nonlocality in a reorientational medium.

We are grateful to A. De Luca and C. Umeton (University of Calabria, Italy) for providing the LC samples. C.C. acknowledges the Tronchetti Provera Foundation for a generous grant. This work was supported by INFM (Advanced Research Project "SPASONELIC").

- [1] *Spatial Solitons*, edited by S. Trillo and Torruellas (Springer-Verlag, Berlin, 2001).
- [2] V.V. Konotop and M. Salerno, *Phys. Rev. A* **65**, 021602 (2002).
- [3] S. Barland *et al.*, *Nature (London)* **419**, 699 (2002).
- [4] A. Hasegawa, *Opt. Lett.* **9**, 288 (1984).
- [5] T.B. Benjamin and J.E. Feir, *J. Fluid Mech.* **27**, 417 (1967).
- [6] D. Grozev, A. Shivarova, and S. Tanev, *J. Plasma Phys.* **45**, 297 (1991).
- [7] D. Grozev, K. Kirov, K. Makasheva, and A. Shivarova, *IEEE Trans. Plasma Sci.* **25**, 415 (1997).
- [8] A.J. Campillo, S.L. Shapiro, and B.R. Suydam, *Appl. Phys. Lett.* **23**, 628 (1973).
- [9] A.V. Mamaev, M. Saffman, and A.A. Zozulya, *Phys. Rev. Lett.* **76**, 2262 (1996).
- [10] D. Kip, M. Soljajic, M. Segev, E. Eugenieva, and D.N. Christodoulides, *Science* **290**, 495 (2000).
- [11] J. Klinger, H. Martin, and Z. Chen, *Opt. Lett.* **26**, 271 (2001).
- [12] R. Malendevich, L. Jankovic, G. Stegeman, and J.S. Aitchison, *Opt. Lett.* **26**, 1879 (2001).
- [13] R.A. Fuerst, D.M. Baboiu, B. Lawrence, W.E. Torruellas, G.I. Stegeman, S. Trillo, and S. Wabnitz, *Phys. Rev. Lett.* **78**, 2756 (1997).
- [14] H. Fang, R. Malendevich, R. Schiek, and G.I. Stegeman, *Opt. Lett.* **25**, 1786 (2000).
- [15] R. Schiek, H. Fang, R. Malendevich, and G.I. Stegeman, *Phys. Rev. Lett.* **86**, 4528 (2001).
- [16] G.I. Stegeman, R. Schiek, H. Fang, R. Malendevich, L. Jankovic, L. Torner, W. Sohler, and G. Schreiber, *Laser Phys.* **13**, 137 (2003).
- [17] A.G. Litvak, V.A. Mironov, G.M. Fraiman, and A.D. Yunakovskii, *J. Plasma Phys.* **1**, 31 (1975).
- [18] A.W. Snyder and D.J. Mitchell, *Science* **276**, 1538 (1997).
- [19] G.C. Duree, J.L. Shultz, G.J. Salamo, M. Segev, A. Yariv, B. Crosignani, P. DiPorto, E.J. Sharp, and R.R. Neurgaonkar, *Phys. Rev. Lett.* **71**, 533 (1993).
- [20] A.V. Mamaev, A.A. Zozulya, V.K. Mezentsev, D.Z. Anderson, and M. Saffman, *Phys. Rev. A* **56**, R1110 (1997).
- [21] E. DelRe, A. Ciattoni, and A.J. Agranat, *Opt. Lett.* **26**, 908 (2001).
- [22] A. Dreischuh, G.G. Paulus, F. Zacher, F. Grasbon, and H. Walther, *Phys. Rev. E* **60**, 6111 (1999).
- [23] F. Henninot, M. Debailleul, and M. Warenghem, *Mol. Cryst. Liq. Cryst. Sci. Technol., Sect. A* **375**, 631 (2002).
- [24] M. Peccianti and G. Assanto, *Phys. Rev. E* **65**, 035603 (2002).
- [25] A. Parola, L. Salasnich, and L. Reatto, *Phys. Rev. A* **57**, R3180 (1998).
- [26] V.M. Perez-Garcia, V.V. Konotop, and J.J. Garcia-Ripoll, *Phys. Rev. E* **62**, 4300 (2000).
- [27] W. Krolikowski, O. Bang, J.J. Rasmussen, and J. Wyller, *Phys. Rev. E* **64**, 016612 (2001).
- [28] J. Wyller, W. Krolikowski, O. Bang, and J.J. Rasmussen, *Phys. Rev. E* **66**, 066615 (2002).
- [29] N.V. Tabirian, A.V. Sukhov, and B.Y. Zel'dovich, *Mol. Cryst. Liq. Cryst.* **136**, 1 (1986).
- [30] I.C. Khoo, *Liquid Crystals: Physical Properties and Nonlinear Optical Phenomena* (Wiley, New York, 1995).
- [31] C. Conti, M. Peccianti, and G. Assanto, *Phys. Rev. Lett.* (to be published).